

High-resolution photoluminescence spectrum of $\text{GdVO}_4:\text{Eu}^{3+}$ ☆

Qing-li Zhang^{a,b}, Chang-xin Guo^{a,b}, Chao-shu Shi^{a,b,*}, Shao-zhe Lü^c

^aStructure Research Lab., University of Science and Technology of China, 230026, Hefei, China

^bDepartment of Physics, University of Science and Technology of China, 230026, Hefei, China

^cOpen Laboratory of Changchun Institute of Physics, Academia Sinica, 130021, Changchun, China

Received 4 February 2000; accepted 26 May 2000

Abstract

In this article, the high-resolution photoluminescence spectrum of $\text{GdVO}_4:\text{Eu}^{3+}$ was studied. The result indicates that Eu^{3+} in $\text{GdVO}_4:\text{Eu}^{3+}$ replaces Gd^{3+} and occupies D_{2d} symmetry, the position 4a (000) of the space group $I4/amd$. The decay times of the $^5D_0 \rightarrow ^7F_2$ and $^5D_1 \rightarrow ^7F_1$ emissions of Eu^{3+} in $\text{GdVO}_4:\text{Eu}^{3+}$ were measured, they are 0.44 ms and 10.7 μs , respectively. The infrared spectrum of $\text{GdVO}_4:\text{Eu}^{3+}$ consists of two peaks at 843.54 and 451.45 cm^{-1} and indicates that an Eu^{3+} in the state 5D_1 can relax to the state 5D_0 by emitting two phonons. © 2000 Elsevier Science S.A. All rights reserved.

Keywords: $\text{GdVO}_4:\text{Eu}^{3+}$; Photoluminescence; High-resolution spectrum; Decay time; Infrared spectrum

PACS: 78.55

1. Introduction

GdVO_4 is an excellent laser medium. It has attracted great interest recently. The studies of GdVO_4 doped with rare earth ions Pr^{3+} , Nd^{3+} , Eu^{3+} , Ho^{3+} , Er^{3+} , Tm^{3+} and Yb^{3+} have been reported [1–7]. $\text{GdVO}_4:\text{Eu}^{3+}$ is an interesting red-emitting material [5–7]; its most important application would be as a laser material. Because of a strong absorption to ultraviolet light by GdVO_4 , an effective energy transfer from VO_4^{3-} to Eu^{3+} and effective excitation of Eu^{3+} by the 450-nm strong emission of VO_4^{3-} , $\text{GdVO}_4:\text{Eu}^{3+}$ is a highly efficient red-emitting material. Under 253.7-nm excitation, $\text{YVO}_4:\text{Eu}^{3+}$, $\text{LuVO}_4:\text{Eu}^{3+}$, $\text{Y}_2\text{O}_3:\text{Eu}^{3+}$ and $\text{GdVO}_4:\text{Eu}^{3+}$ has almost equal emission intensity. At the same time, we found that $\text{GdVO}_4:\text{Eu}^{3+}$ has a very good temperature property, from a few K to room temperature its principal emission has no obvious change, above the room temperature, its principal emission increases with increasing temperature and by more than one order at about 600 K. Thus, it can be used in high-pressure mercury light etc. The principal emission peak of $\text{GdVO}_4:\text{Eu}^{3+}$ is 619 nm, according to our calculation,

its colourity coordinates are $x=0.67$ and $y=0.32$. It can be used as trichromatic material.

Some luminescence properties of $\text{GdVO}_4:\text{Eu}^{3+}$ have been reported [5,6], but its high-resolution photoluminescence of 0.15 cm^{-1} and by which the symmetry of Eu^{3+} replacing Gd^{3+} in the lattice is shown. Infrared spectrum and decay time of Eu^{3+} emission have not been reported before to our knowledge. In this article, these properties are studied.

GdVO_4 has ZrSiO_4 structure, belonging to the space group $I4/amd$ (Gd^{3+} , V^{5+} and O^{2-} occupy the positions 4a(0 0 0), 4b(0 0 0.5) and 16h(0 x z), respectively) [8]. It is tetragonal system and its lattice parameters are $a=7.2176$ Å, $c=6.3483$ Å, $Z=4$, $D_x=5.474$ g/cm³ [9].

2. Experiments

The polycrystalline sample of $\text{GdVO}_4:\text{Eu}^{3+}$ was prepared by reacting stoichiometric proportions of V_2O_5 and Gd_2O_3 with purity 99.99 and 99.95%, respectively, and the nitric acid solution of Eu_2O_3 was used to dope Eu^{3+} into GdVO_4 . The stoichiometric mixture was sintered in air atmosphere at 800°C for 8 h and the polycrystalline $\text{GdVO}_4:\text{Eu}^{3+}$ was obtained.

In order to determine the crystal structure of GdVO_4 ,

☆Supported by NSFC of China under Grant No. 59732040.

*Corresponding author.

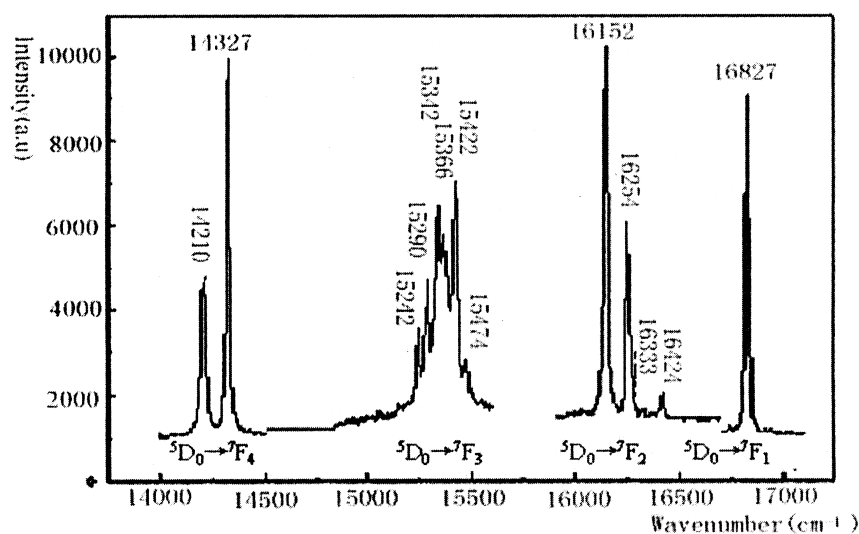
E-mail address: shics@utsc.edu.cn (C.-s. Shi).

its X-ray diffraction measurement was performed at room temperature using a D/Mrax-rA Rotating Anode X-ray Diffractometer with $\text{CuK}\alpha$ radiation. The position and intensity of diffraction peaks of the polycrystalline powder GdVO_4 are consistent with that of the powder diffraction file (PDF) 17-260, which indicates that the sample crystallized well. From the experimental data, the lattice parameters $a=7.22\text{\AA}$ and $c=6.38\text{\AA}$ were calculated with the least square method. From the formula $D_x=1.66ZM_r/V$ (where V and Z are the volume and number of molecules of a primitive unit cell, M_r is the molecular weight, respectively), the density of GdVO_4 , $D_x=5.46\text{ (g/cm}^3\text{)}$ was calculated and consistent with the D_x data of PDF 17-260.

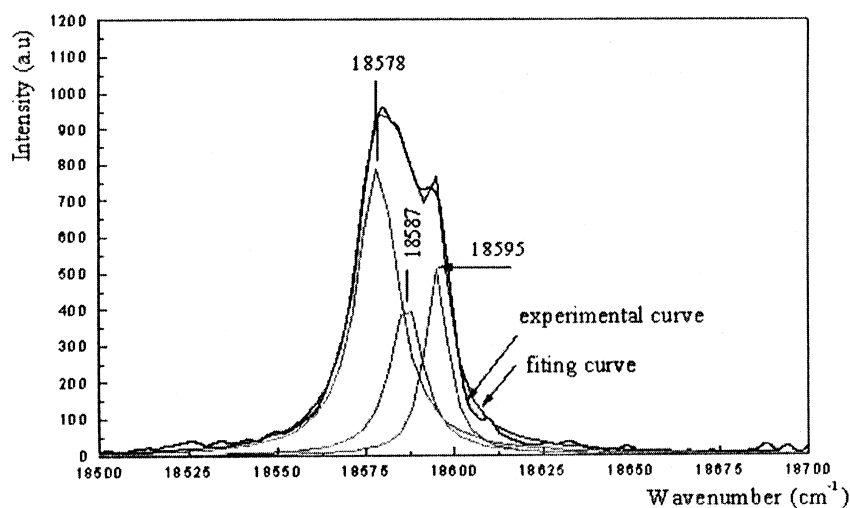
The high-resolution photoluminescence of $\text{GdVO}_4:\text{Eu}^{3+}$ was excited by the 266-nm laser line of the fourth order output of a GCR-2A YAG:Nd laser. The monochromator, with resolution 0.15 cm^{-1} , is a SPEX-1403 double raster monochromator of SPEX corporation. The high-resolution photoluminescence spectrum is shown in Fig. 1.

The luminescence decay times of Eu^{3+} in $\text{GdVO}_4:\text{Eu}^{3+}$ were measured at room temperature using a 162 BOX-CAR.

The infrared spectrum of $\text{GdVO}_4:\text{Eu}^{3+}$ was performed on a Fourier Transform Infrared Spectrometer of Nicolet Instrument. Its maximal resolution is 0.1 cm^{-1} and accuracy is superior to 0.01 cm^{-1} . Before measuring, the mixture of $\text{GdVO}_4:\text{Eu}^{3+}$ and KBr with fluorescence purity was



(a)



(b)

Fig. 1. High-resolution photoluminescence spectrum from (a) $^5\text{D}_0 \rightarrow ^7\text{F}_J$ ($J=1, 2, 3, 4$) transition and (b) $^5\text{D}_1 \rightarrow ^7\text{F}_1$ transition of $\text{GdVO}_4:\text{Eu}^{3+}$ (10 mol%) ($\lambda_{\text{ex}}=266\text{ nm}$).

Table 1

Lineshape fitting parameters of the spectrum curve of $^5D_1 \rightarrow ^7F_1$ transition of Eu^{3+} in GdVO_4

Spectrum line center (cm^{-1})	Width (cm^{-1})	Height (a.u)
18 578	14.3	787.5
18 587	11.3	423.4
18 595	7.8	514.1

ground in an agate, then, the mixture was pressed into a disk with a tablet machine and was measured.

3. Experimental results and discussion

3.1. High-resolution photoluminescence spectrum of $\text{GdVO}_4:\text{Eu}^{3+}$

The high-resolution photoluminescence spectrum (HRPLS) of $\text{GdVO}_4:\text{Eu}^{3+}$ is shown in Fig. 1. The spectrum shape of $^5D_1 \rightarrow ^7F_1$ transition of Eu^{3+} was fitted with Lorentz lineshape, as shown in Fig. 1b and the fitting parameters are listed in Table 1. If the spectrum curve is fitted with Guass lineshape, there will be a very wide and flat peak, which does not seem reasonable. The lineshape of the $^5D_1 \rightarrow ^7F_1$ transition is a Lorentz lineshape, which maybe indicate that the linear broadening in $\text{GdVO}_4:\text{Eu}^{3+}$ was mainly caused by thermal vibration of the lattice.

Because Gd^{3+} and Eu^{3+} are neighbor elements on the

periodic table, their ion radii are 0.95 and 0.94 Å, respectively. It is commonly suggested that Eu^{3+} replaces Gd^{3+} in $\text{GdVO}_4:\text{Eu}^{3+}$. After replacing Gd^{3+} , Eu^{3+} will be surrounded by eight O^{2-} and has D_{2d} symmetry, which results in energy level splitting of Eu^{3+} and the photoluminescence spectrum of Eu^{3+} will be obviously different from that of Eu^{3+} in the crystal fields belonging to the other symmetry. Calculated by crystal field theory [10,11], the energy level splitting of Eu^{3+} in symmetry D_{2d} was shown in Tables 2 and 3. In Tables 2 and 3, the theoretical and experimental $^5D_0 \rightarrow ^7F_J$ ($J=1, 2, 3, 4$) and $^5D_1 \rightarrow ^7F_1$ transition values also have been listed.

From Tables 1 and 2 it can be seen that the observed lines are consistent with the calculated lines very well, except that the lines 14 275, 14 375 cm^{-1} of $^5D_0 \rightarrow ^7F_4$ transition and 16 843 cm^{-1} of $^5D_0 \rightarrow ^7F_1$ transition are too weak to emerge.

The lines 16 424 and 16 333 cm^{-1} near the $^5D_0 \rightarrow ^7F_2$ transition of Eu^{3+} are from $^5D_2 \rightarrow ^7F_6$ transition of Eu^{3+} . The lines 15 366, 15 422 and 15 474 cm^{-1} near the $^5D_0 \rightarrow ^7F_3$ transition of Eu^{3+} are from the $^4G_{5/2} \rightarrow ^6H_{9/2}$ transition of Sm^{3+} , which exists as the impurity in Eu_2O_3 . Because of the high concentration of Eu^{3+} , it is possible that a small amount of Sm^{3+} was taken into the sample from Eu_2O_3 . On the other hand, $^5D_0 \rightarrow ^7F_3$ emission of Eu^{3+} is very weak, so even if the principal emission of Sm^{3+} is very weak, they have almost equal intensity and can be detected at the same time.

As shown in Fig. 2, the photoluminescence spectrum

Table 2

Energy level 7F_J and $^5D_0 \rightarrow ^7F_J$ transition of Eu^{3+} in D_{2d} symmetry in GdVO_4 ^{a,b}

J	Γ	Energy level (cm^{-1})	$^5D_0 \rightarrow ^7F_J$ transition			
			ED	MD	Experimental values (cm^{-1})	Calculated values (cm^{-1})
0	A_1		–	–		
1	A_2	350	–	+	Too weak to emerge	16 843
	E	368	+	+	16 827	16 825
2	B_1	1122	–	–		
	E	1044	+	+	16 152	16 149
	A_1	993	–	–		
	B_2	935	+	–	16 254	16 258
3	E	1954	+	+	15 242	15 239
	B_1	1910	–	–		
	A_2	1906	–	+	15 290	15 287
	E	1864	+	+	15 342	15 329
	B_2	1854	+	–	15 342	15 339
4	A_1	3062	–	–		
	E	2987	+	+	14 210	14 206
	A_2	2918	–	+	Too weak to emerge	14 275
	A_1	2884	–	–		
	B_2	2866	+	–	14 327	14 326
	E	2818	+	+	Too weak to emerge	14 375
	B_1	2701				

^a G, ED and MD stand for unreducible representation, electronic and magnetic dipole transition, respectively. + and – stand for transition permitted and forbidden. The energy level 5D_0 is 17 193 cm^{-1} .

^b Refs. [10,11].

Table 3

 $^5D_1 \rightarrow ^7F_1$ transition of Eu^{3+} in D_{2d} symmetry in GdVO_4 ^{ab}

Initial state energy level (cm^{-1})		Final state energy level (cm^{-1})		$^5D_1 \rightarrow ^7F_1$ transition	
5D_1		7D_1		Experimental values (cm^{-1})	Calculated values (cm^{-1})
A_2	18 947	A_2	368	—	
		E	350	18 587	18 597
E	18 949	A_2	368	18 578	18 581
		E	350	18 595	18 599

^a Where ‘—’ stands for the transition forbidden.^b Refs. [11,12].

(PLS) of $\text{GdVO}_4:\text{Eu}^{3+}$ and $\text{GdVO}_4:\text{Sm}^{3+}$ was measured with a 850 fluorescence spectrophotometer of HITACHI corporation.

From the photoluminescence spectrum of $\text{GdVO}_4:\text{Sm}^{3+}$ (Fig. 2b), it can be seen that the strongest emission of $\text{GdVO}_4:\text{Sm}^{3+}$ peaks at about 603.7, 606.8 and 646.4, 654.6 nm, which are from $^4G_{5/2} \rightarrow ^6H_{7/2}$ and $^4G_{5/2} \rightarrow ^6H_{9/2}$ transitions of Sm^{3+} , respectively. The Sm^{3+} lines emerging in HRPLS of $\text{GdVO}_4:\text{Eu}^{3+}$ (Fig. 1a) are the lines 650.8, 648.4 and 646.3 nm (15 366, 15 422 and 15 474 cm^{-1} , respectively), corresponding to the lines 654.6 and 646.4 nm of PLS of $\text{GdVO}_4:\text{Sm}^{3+}$, respectively. We can see that the lines 650.8 and 648.4 nm of HRPLS were not discerned by the 850 fluorescence spectrophotometer. They correspond to the same line at 654.6 nm in PLS of $\text{GdVO}_4:\text{Sm}^{3+}$. Because the luminescence efficiency of $\text{GdVO}_4:\text{Sm}^{3+}$ is not so high that the slits of the fluorescence spectrophotometer can not be opened very narrowly, which results in the two lines not been discerned by the 850 fluorescence spectrophotometer. The lines of $\text{GdVO}_4:\text{Sm}^{3+}$ in HRPLS and in PLS are very consistent,

so we can conclude that the lines 15 366, 15 422 and 15 474 cm^{-1} are from the emission of the impurity Sm^{3+} .

If the symmetry of Eu^{3+} is D_{2d} , its 580-nm emission from $^5D_0 \rightarrow ^7F_0$ transition is forbidden as for magnetic or electronic dipole transition. It is consistent with the results shown in Fig. 2, the 580 nm (that is 17 241 cm^{-1}) transition didn't emerge.

From the above, it can be concluded that Eu^{3+} replaces Gd^{3+} , has D_{2d} symmetry and occupies the position 4a(0 0 0) of the space group $I4/amd$.

3.2. Luminescence decay time of $\text{GdVO}_4:\text{Eu}^{3+}$

The luminescence decay curves of $\text{GdVO}_4:\text{Eu}^{3+}$ are shown in Fig. 3 (solid curves), which were fitted by $I = I_0 \exp(-t/\tau)$ (where I_0 and t denote initial luminescence intensity and the time when luminescence intensity decays to I_0/e , the fitting curves are dot curves). The fitting parameters are listed in Table 4. The decay times of $^5D_0 \rightarrow ^7F_2$ and $^5D_1 \rightarrow ^7F_1$ emissions are 0.44 ms and 10.72 μs , respectively. From the exponent decay law of the

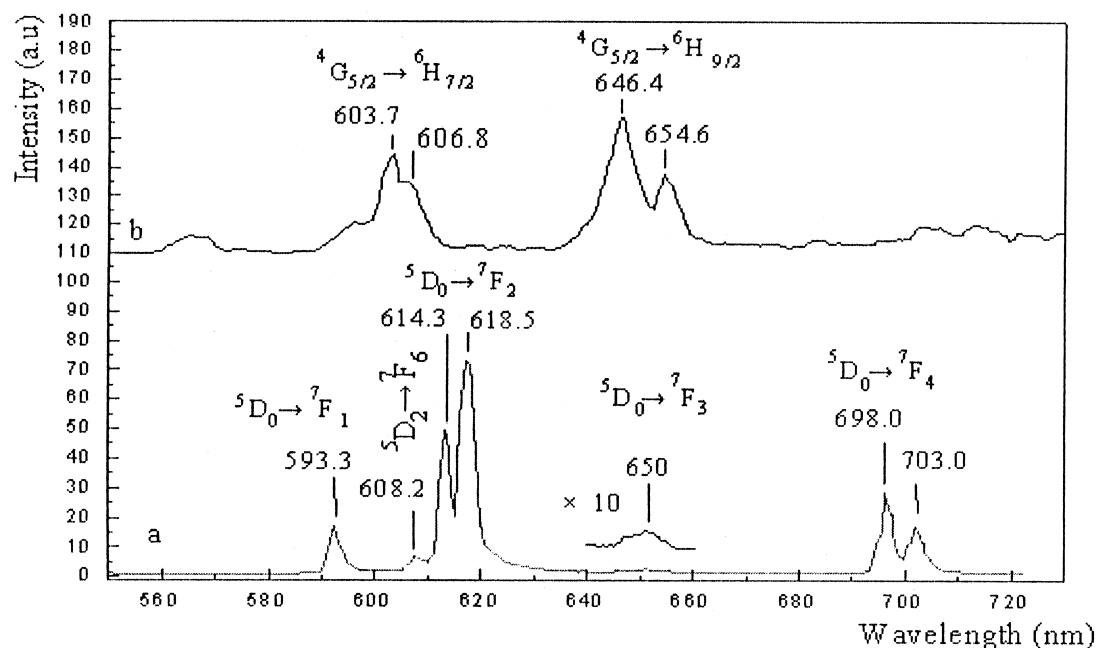


Fig. 2. Photoluminescence spectrum of (a) $\text{GdVO}_4:\text{Eu}^{3+}$ (10 mol %) and (b) $\text{GdVO}_4:\text{Sm}^{3+}$ (1 mol %) ($\lambda_{\text{ex}} = 310 \text{ nm}$).

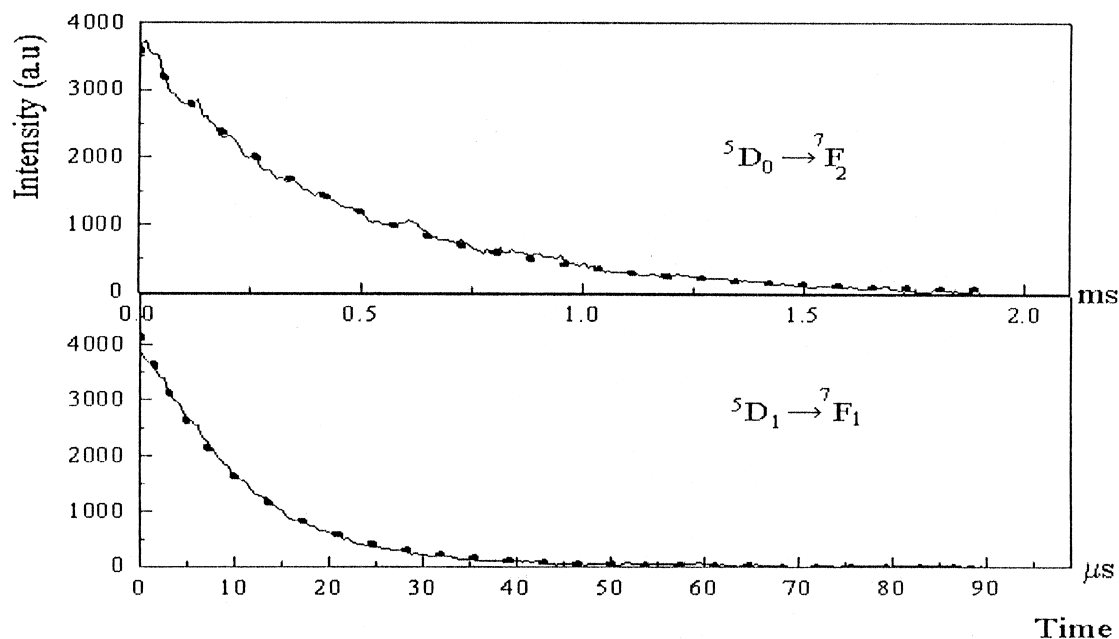


Fig. 3. Luminescence decay curves of $^5D_1 \rightarrow ^7F_1$ and $^5D_0 \rightarrow ^7F_2$ emissions of $GdVO_4:Eu^{3+}$ (10 mol %) ($\lambda_{ex} = 266$ nm). In the figure, solid and dot curves are experimental and fitting curves, respectively.

emission, Eu^{3+} in $GdVO_4:Eu^{3+}$ is an isolated luminescence center.

But the decay time of $^5D_1 \rightarrow ^7F_1$ emission is more than 40 times faster than that of the $^5D_0 \rightarrow ^7F_2$ emission, due to the interaction between Eu^{3+} and lattice. A rare earth ion in an excited state i decays with a mean lifetime τ_i given by

$$\frac{1}{\tau_i} = \sum_j (A_{ij} + W_{ij})$$

where A and W are the probabilities for radiative and nonradiative decay, respectively, and the summation is over all terminal states j . A and W are the functions of energy difference [13,14]. For J manifolds separated by small energy gaps, $\sum W_{ij}$ is usually much greater than $\sum A_{ij}$. With respect to the energy level 5D_1 of Eu^{3+} , there is an energy level 5D_0 , which is only 1740 cm^{-1} below it, so through the interaction with the lattice, the excited state 5D_1 can relax to the state 5D_0 through nonradiative transition quickly, which results in the mean lifetime of 5D_0 being very short. As for the excited state 5D_0 , the nearest energy level below it is 7F_6 , the energy difference

between 5D_0 and 7F_6 state is 16155 cm^{-1} , which is far greater than the energy of a phonon, this results in it being hardly possible that the multiphonon transition from $^5D_0 \rightarrow ^7F_6$ occurs, so nonradiative transition probability $\sum W_{ij} < \sum A_{ij}$, the mean lifetime of the excited state 5D_0 becomes long.

3.3. Infrared transmission spectrum of $GdVO_4:Eu^{3+}$

The infrared spectrum of $GdVO_4:Eu^{3+}$ is shown in Fig. 4. There are two peaks at 834.54 and 451.45 cm^{-1} . Through a Fourier self-deconvolution method program, which is provided by the software of Nicolet Instrument, the peak at 834.54 cm^{-1} was decomposed into seven peaks, which are at 949.89 , 881.57 , 856.15 , 834.90 , 808.59 , 785.66 and 770.44 cm^{-1} , respectively, as shown in the small box of the Fig. 4. These peaks show the absorption of the lattice phonon. In $GdVO_4:Eu^{3+}$, the energy difference between 5D_0 and 5D_1 is 1740 cm^{-1} , which is double 870 cm^{-1} and in the range of $949.89 - 770.44 \text{ cm}^{-1}$. So in $GdVO_4:Eu$, an electron in the state 5D_1 can relax to the state 5D_0 quickly by emitting two phonons of about 870 cm^{-1} .

Table 4

Fitting parameters of luminescence decay curves of $^5D_1 \rightarrow ^7F_1$ and $^5D_0 \rightarrow ^7F_2$ emissions^a

	$^5D_1 \rightarrow ^7F_1$	$^5D_0 \rightarrow ^7F_2$
I_0 (a.u.)	4158.6	3628.4
τ (μ s)	10.72	0.44

^a I_0 , τ are initial luminescent intensity and the time when luminescence intensity decays to $I = I_0/e$, respectively.

4. Conclusion

1. The high-resolution photoluminescence spectrum of $GdVO_4:Eu^{3+}$ indicates that Eu^{3+} replaces Gd^{3+} , has D_{2d} symmetry and occupies the position $4a(0\ 0\ 0)$ of the space group $I4/amd$.

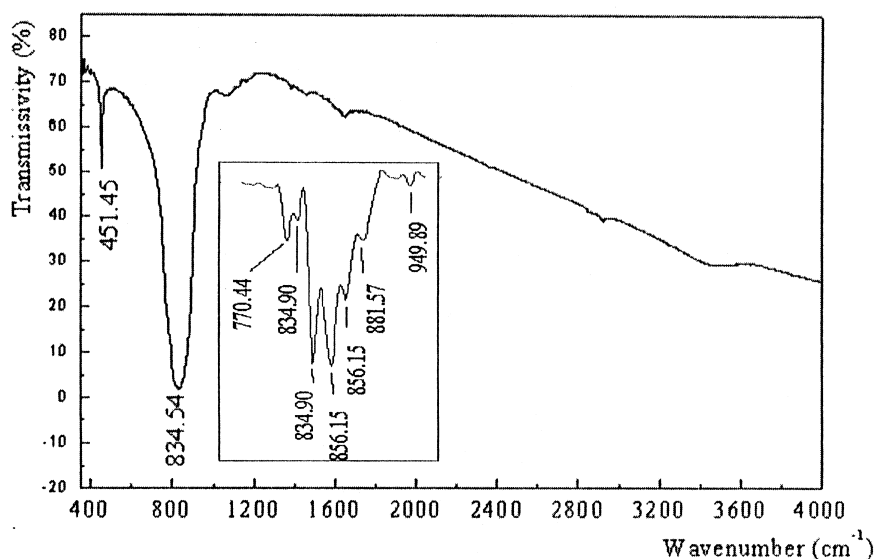


Fig. 4. Infrared spectrum of $\text{GdVO}_4:\text{Eu}^{3+}$ (10 mol%). The curve in the small box of the figure is the peaks obtained by decomposing the peak 834.54 cm^{-1} with the Fourier self-deconvolution method.

2. The decay times of $^5\text{D}_0 \rightarrow ^7\text{F}_2$ and $^5\text{D}_1 \rightarrow ^7\text{F}_1$ emissions of Eu^{3+} in $\text{GdVO}_4:\text{Eu}^{3+}$ (10 mol %) are 0.44 ms and 10.7 μs , respectively. The difference is due to different reactions with the lattice of the excited states $^5\text{D}_0$ and $^5\text{D}_1$ of Eu^{3+} .
3. The infrared spectrum of $\text{GdVO}_4:\text{Eu}^{3+}$ consists of two peaks at 843.54 and 451.45 cm^{-1} and indicates that an Eu^{3+} in $^5\text{D}_1$ state can relax to $^5\text{D}_0$ state by emitting two phonons quickly.

References

- [1] P.A. Studenikin, A.I. Zagumennyi, Yu.D. Zavartsev, P.A. Popov, I.A. Shcherbakov, *Quantum Electron (UK)* 25 (1995) 1162.
- [2] A.I. Zagumennyi, T.D. Zavartsev, P.A. Studenikin, I.A. Scherbakov, F. Umyskov, *Proc. SPIE. Int. Soc. Opt. Eng. (USA)* 2698 (1996) 182.
- [3] V.A. Mikhailov, Yu.D. Zavartsev, A.I. Zagumennyi, *Quantum Electron (UK)* 27 (1997) 13.
- [4] E. Antic-Fidancev, M. Lemaitre-Blaise, P. Porcher, *Spectrochim. Acta (Part A)* 54A (1998) 2151.
- [5] A. Bril, W.L. Wanmaker, J. Bross, *J. Chem. Phys.* 43 (1965) 311.
- [6] L.H. Brixner, E. Abramson, *J. Electrochem. Soc.* 112 (1965) 70.
- [7] F.C. Palilla, A.K. Levin, M. Rinkevics, *J. Electrochem. Soc.* 112 (1965) 776.
- [8] H. Fuess, A. Kallel, *J. Solid State Chem.* 5 (1972) 11.
- [9] The Joint Committee on Powder Diffraction Standards, *Powder Diffraction File Sets 16 to 18*, No. 17–260, Philadelphia, 1974, p. 353.
- [10] S. Qiang, in: *Chemistry of Rare Earth*, Press of Science and Technology of Henan, Henan, 1993, p. 305, in Chinese.
- [11] C. Linares, A. Louat, M. Blandchard, *Struct. Bonding* 33 (1977) 179.
- [12] C. Brecher, H. Samelson, A. Lempicki, The energy level structure of Eu^{3+} in YVO_4 , in: H.M. Crosswhite, H.W. Moos (Eds.), *Optical Properties of Ions in Crystals*, Interscience Publishers, New York, 1967, p. 73.
- [13] G.H. Dieke, L.A. Hall, *J. Chem. Phys.* 27 (1957) 465.
- [14] M.J. Weber, *Phys. Rev. B* 8 (1973) 54.